bioRxiv preprint doi: https://doi.org/10.1101/389361; this version posted August 10, 2018. The copyright holder for this preprint (which was not certified by peer review) is the author/funder, who has granted bioRxiv a license to display the preprint in perpetuity. It is made available under aCC-BY-NC-ND 4.0 International license.

Development of whole-porcine monoclonal antibodies with potent neutralization activity against classical swine fever virus (CSFV) from single B cells

Haisi Dong,[a] Dongmei Lv,[a] Ang Su,[a] Lerong Ma,[a] Jianwei Dong,[a] Nannan Guo,[a] Linzhu Ren,[a] Huping Jiao,[a] Daxin Pang,[a]# Hongsheng Ouyang[a]#

[a]Jilin Provincial Key Laboratory of Animal Embryo Engineering, College of Animal Science, Jilin University, Changchun, Jilin Province, People's Republic of China

Running Head: Isolation of monoclonal antibodies against CSFV from single B cells

#Address correspondence to: Hongsheng Ouyang (ouyh@jlu.edu.cn) and Daxin Pang, (pdx@jlu.edu.cn)

Haisi Dong and Dongmei Lv contributed equally to this work.

*Present address: Jilin Provincial Key Laboratory of Animal Embryo Engineering, College of Animal Science, Jilin University, 5333 Xi'an Road, Lvyuan District, Changchun 130062, Jilin Province, People's Republic of China.

Abstract: 219 words

Text: 5616 words

bioRxiv preprint doi: https://doi.org/10.1101/389361; this version posted August 10, 2018. The copyright holder for this preprint (which was not certified by peer review) is the author/funder, who has granted bioRxiv a license to display the preprint in perpetuity. It is made available under aCC-BY-NC-ND 4.0 International license.

Abstract (max 250 words, currently 219)

Classical swine fever (CSF) is a highly contagious swine disease found worldwide that has caused devastating economic losses. However, there are few efficacious mAbs against the CSF virus (CSFV) that can be used for treatment because most mAbs against CSFV are derived from mouse hybridoma cells and these murine mAbs have disadvantages of inefficient effector functions elicitations and high immunogenicity *in vivo*. Accordingly, we characterized whole-porcine anti-CSFV neutralizing mAbs (NAbs) isolated directly from single B cells sorted from a CSFV-vaccinated pig using the fluoresceinated conserved linear neutralizing epitope of the CSFV E2 protein and fluorophore conjugated goat anti-pig IgG. Immunoglobulin (Ig) genes were isolated via nested PCR, and two porcine mAbs termed HK24 and HK44 were produced. We determined that these mAbs can bind to E2 protein and recognize sites within this major antigenic epitope. In addition, we found that mAbs HK24 and HK44 exhibit potent neutralizing activity against CSFV, and they can protect PK-15 cells from infections *in vitro* with potent IC_{50} values of 9.3 μg/ml and 0.62 μg/ml, respectively. Notably, we demonstrated that these two mAbs can be used as novel reagents for detecting virus infection. These data suggest that our results not only provide a method for efficiently obtaining mAbs against CSFV but also offer promising mAb candidates for development of antibody-based diagnostic and antiviral agents.

Keywords: Classical swine fever; epitope of E2 protein; whole-porcine anti-CSFV neutralizing mAbs; single B cells;

bioRxiv preprint doi: https://doi.org/10.1101/389361; this version posted August 10, 2018. The copyright holder for this preprint (which was not certified by peer review) is the author/funder, who has granted bioRxiv a license to display the preprint in perpetuity. It is made available under aCC-BY-NC-ND 4.0 International license.

38 **Importance (max 150 words, currently 123)**

39 Neutralizing monoclonal antibodies (NAbs) can prevent and may slow the spread of virus
40 infection. The discovery of NAbs that recognize classical swine fever virus (CSFV)
41 necessitates new technologies because the NAbs produced by immunization and hybridoma
42 technology could not be transferred to *in vivo* research. Multiple full-length human
43 therapeutic antibodies have been produced via single-cell polymerase chain reactions but
44 whole-porcine NAbs for CSFV have not been generated. In this study, two whole-porcine
45 mAbs, named HK24 and HK44, were isolated from epitope-specific single B cells. We
46 demonstrate that these two mAbs have potent neutralizing activity against CSFV and can
47 protect cells against viral infection. Therefore, they may facilitate the development of
48 vaccines or antiviral drugs that offer the advantages of stability and low immunogenicity.

49

bioRxiv preprint doi: https://doi.org/10.1101/389361; this version posted August 10, 2018. The copyright holder for this preprint (which was not certified by peer review) is the author/funder, who has granted bioRxiv a license to display the preprint in perpetuity. It is made available under aCC-BY-NC-ND 4.0 International license.

Introduction

Classical swine fever (CSF) caused by classical swine fever virus (CSFV) is a highly contagious and fatal viral swine disease that remains a serious problem for the pork industry (1-3). CSFV is an enveloped virus with positive-sense RNA and belongs to the genus *Pestivirus* of the family *Flaviviridae* (4). The mature CSFV virion contains twelve viral proteins, N^{pro}, C, E^{rns}, E1, E2, p7, NS2, NS3, NS4A, NS4B, NS5A, and NS5B (5). E2 is a protein with multiple functions that can form a dimer with E1 and mediate virion entry into target cells; additionally, it is the major antigen for the production of neutralizing antibodies that protect the body from the virus. The ability of an anti-E2 antibody to neutralize CSFV has previously been characterized in detail (6, 7). The E2 protein consists of four antigen domains, A, B, C, and D, at the N-terminus with a total of 177 amino acids, ranging from amino acids 690 to 866. These domains contain some conformational epitopes and linear epitopes that play critical roles in inducing neutralizing antibodies. Comparison of the different epitopes of the E2 protein has demonstrated that the linear epitope CTAVSPTTLRTEVVK, found between amino acids 828 and 842, a region recognized by the monoclonal antibody WH303, is strongly conserved in different CSFV strains but is highly divergent among bovine virus diarrhoea virus (BVDV) and border disease virus (BDV) strains (8, 9).

NAbs that are capable of directly neutralizing most strains of a given highly antigenic variable pathogen have attracted considerable attention because they can used to treat some of the difficult infectious diseases encountered in modern medicine and have potential for development of passive immunotherapy treatment or vaccine reagents (10). In addition, given their potential antiviral effects, NAbs also play an essential role in studying the structure-function properties of infectious agents and related pathogenesis. However, mAbs of mouse origin that are produced by hybridoma technology cannot be applied in *in vivo* research because they can induce the production of anti-mouse antibodies *in vivo*, leading to a short half-life (11-13). Other traditional methods of generating mAbs, such as Epstein-Barr virus-transformation and phage-display libraries, are limited by being unstable, time consuming or inefficient (14, 15). With the advent of single-cell reverse transcription PCR (RT-PCR) technologies, the amplification of full-length immunoglobulin gene (Ig) fragments from single B cells by utilizing nested PCR has allowed the bypass of many of these limitations and this technology has been shown to provide a versatile tools for generation of new mAbs; this is an important advancement in mAbs production (16, 17). Prior to the amplification of Ig-encoding genes, antigen-specific memory B cells must be stained with fluorescently-labelled antigen baits and then sorted. Several human mAbs against HIV, ZIKV and Ebola virus have been obtained through this technology (18-20). However, the production of whole-porcine mAbs against the E2 protein of CSFV using linear specific-epitopes has not been reported. Whole-porcine neutralizing antibodies usually exhibit the lowest immunogenicity, longer half-lives and have a great potential for superior applications in *in vivo* (21, 22).

In this study, we report the acquisition of the whole-porcine mAbs HK24 and HK44. These mAbs were isolated from single B cells of a vaccinated pig using the fluoresceinated epitope CTAVSPTTLRTEVVK and fluorescein isothiocyanate (FITC)-labelled goat anti-pig IgG via fluorescent-activated cell sorting (FACS) (23). Their ability to significantly neutralize CSFV was identified through a panel of assays. We also confirmed that these mAbs

bioRxiv preprint doi: https://doi.org/10.1101/389361; this version posted August 10, 2018. The copyright holder for this preprint (which was not certified by peer review) is the author/funder, who has granted bioRxiv a license to display the preprint in perpetuity. It is made available under aCC-BY-NC-ND 4.0 International license.

94 demonstrate significant value for the serological diagnosis of CSFV infection. Together, the
95 porcine mAbs HK24 and HK44 show potential as candidates for immunotherapy or
96 diagnostic reagents.
97
98 **Results**
99 **Isolation of single B cells from a vaccinated pig and mAb generation**
100 Individual pigs were immunized with an attenuated vaccine strain of CSFV to generate a
101 spectrum of antibody responses ranging from low to high levels of blocking, which was
102 determined using the Classical Swine Fever Virus Antibody Test Kit (IDEXX, Switzerland);
103 unvaccinated pigs served as negative controls (**Fig. 1A**). As shown in **Fig. 1B**, pigs #3748 and
104 #3757 exhibited a high blocking rate; therefore, blood samples from pig #3748 were used to
105 isolate single B cells that were stained with FITC-conjugated anti-pig IgG and
106 5-TAMRA-conjugated epitope-76 via FACS. Epitope-76 is strongly conserved in different
107 CSFV strains but is highly divergent among the BVDV and BDV strains, as shown in **Fig. 1C**.
108 As shown in **Fig. D**, epitope-specific IgG^+ B cells constituted approximately 0.39% of the cell
109 population. Full-length heavy- and light-chain antibody genes were amplified from the cDNA
110 of single purified B cells via nested PCR and were sequenced. All nine antibodies were
111 obtained from one hundred single epitope-specific IgG^+ B cells. Nucleotide sequence analysis
112 of these genes demonstrated that they could be divided into four different groups. Some of
113 these antibodies shared the same *IgH* and *IgL* genes, and most clones were somatic variants of
114 the IGHV1-4*02 and IGKV1-11*01/IGKV2-10*02 germline genes (**Fig. 1E**). This result was
115 similar to that obtained in a study of ZIKV (20).
116 In summary, we deduced that individuals with high serologic neutralizing titres against
117 the same epitopes of CSFV may express isotype antibodies. We also found that the mAbs
118 HK24 and HK44 each had a long complementarity determining 3 region of anibody
119 heavy-chain (CDR H3) loop composed of 17 and 21 amino acids, respectively. The antibody
120 gene pairs HK24 *IgH*, *IgK* and HK44 *IgH*, *IgK* were selected to produce mAbs, which were
121 identified via SDS-PAGE. Polyclonal antibody IgGs were isolated from porcine serum by
122 protein A were served as a positive control (**Fig. 1F**).
123
124 **The mAbs HK24 and HK44 can bind to specific epitopes of CSFV**
125 To map the epitopes of the mAbs HK24 and HK44, we first checked whether these
126 mAbs react with epitope-76. For this purpose, HEK293T cells were used for the transient
127 expression of mAb HK24 or HK44, and the binding activity of the mAbs HK24 and HK44 to
128 FITC-conjugated epitope-76 (20 μg/ml) was detected and analysed through microscopy. As
129 shown in **Fig. 2A**, there was a high level of green fluorescence in cells transfected with the
130 expression vector for either HK24 or HK44, and cells without expression vectors showed no
131 green fluorescence. This result indicated that HK24 and HK44 could bind to the conserved
132 epitope-76 with a higher affinity. This distinctive feature of the mAbs HK24 and HK44 was
133 further confirmed by flow cytometric analysis, as shown in **Fig. 2B**. FACS results indicated
134 that a higher percentage of HEK293T cells expressing HK24 or HK44 was stained by
135 FITC-conjugated epitope-76 (60.7% and 40.8%, respectively) than HEK293T cells that did
136 not express HK24 and HK44 (0.128%).
137 We also performed a direct fluorescence experiment to ascertain whether the mAbs

bioRxiv preprint doi: https://doi.org/10.1101/389361; this version posted August 10, 2018. The copyright holder for this preprint (which was not certified by peer review) is the author/funder, who has granted bioRxiv a license to display the preprint in perpetuity. It is made available under aCC-BY-NC-ND 4.0 International license.

HK24 or HK44 possess binding specificity to epitope-76. As shown in **Fig. 2C**, the mAbs HK24 and HK44, as well as positive IgGs purified from pig #3748, were recognized efficiently by epitope-76, while HK24 and HK44 did not bind to the unrelated epitope-75 which is a linear epitope on the E2 protein of CSFV. Meanwhile, the positive IgGs interacted efficiently with both epitope-76 and epitope-75.

In summary, these data demonstrated that the mAbs HK24 and HK44 can be specifically recognized by epitope-76 with a high affinity.

The mAbs HK24 and HK44 exhibit high specificity and sensitivity to the CSFV E2 protein

The reactivity between the mAbs and the CSFV E2 protein was deciphered via Western blotting. The results showed that the 55-kDa E2 protein band from lysates of CSFV-infected cells was clearly detected by the mAbs HK24 and HK44 with high specificity, unlike the lysates of uninfected cells (**Fig. 3A and 3B**).

To further verify the reactivity of the mAbs HK24 and HK44 with the CSFV E2 protein, recombinant E2 protein was subsequently produced and used to detect antibody affinity via Western blotting. As expected, the mAbs HK24 and HK44 reacted with recombinant E2 with high specificity (**Fig. 3C**). Indirect ELISA also showed that the mAbs HK24 and HK44 exhibited excellent affinity for the recombinant E2 protein, and binding occurred in a dose-dependent manner, whereas negative IgGs (isolated from CSFV-negative swine serum by protein A) did not show significant reactivity (**Fig. 3D**). Together, these results demonstrated that the mAbs HK24 and HK44 possess specific reactivity with either CSFV E2 protein in cells or purified recombinant E2 protein.

Additionally, to investigate whether the mAbs HK24 and HK44 could be applied for CSFV detection, these antibodies were used to detect CSFV in PK-15 cells via an immunofluorescence assay. As shown in **Fig. 3E**, the mAbs HK24 and HK44 showed strong fluorescence at 30 nM, as observed for CSFV-positive serum, unlike CSFV-negative serum. This result suggested that both mAbs isolated in the present study could be used to detect CSFV. Hence, our results suggested that the mAbs HK24 and HK44 exhibited high sensitivity towards E2 of CSFV and can be used for the serological detection of CSFV infection or for research purposes.

Evaluation of the binding affinity of mAbs HK44 and HK24 to E2 protein by SPR

SPR is a powerful technique that provides affinity and kinetic information for protein-protein interactions (24, 25). Thus, SPR was used to assess the ability of the mAbs HK44 and HK24 to bind the recombinant protein E2. For this purpose, the mAbs HK44 and HK24 were immobilized on CM5 sensor chips with a general 1:1 interaction; the results are shown in **Fig. 4**. As shown in **Fig. 4A and 4B**, SPR dose-dependent binding assays verified that the mAbs HK44 and HK24 bound the E2 protein with high affinity at E2 protein concentrations ranging from 125 nM to 2000 nM. The SPR data indicated that the association rate constant (ka) of the mAbs HK44 and HK24 with the recombinant E2 protein was 1.70×10^4 M^{-1} s^{-1} and 5.01×10^4 M^{-1} s^{-1}, indicating a fast association constant between mAbs HK44 or HK24 and E2 protein and the equilibrium dissociation constant (KD) of 1.85×10^{-7} M and 3.67×10^{-8} M respectively. These results suggest that mAbs HK44 and HK24 exhibit a

bioRxiv preprint doi: https://doi.org/10.1101/389361; this version posted August 10, 2018. The copyright holder for this preprint (which was not certified by peer review) is the author/funder, who has granted bioRxiv a license to display the preprint in perpetuity. It is made available under aCC-BY-NC-ND 4.0 International license.

high binding affinity to the E2 protein. The responses of E2 protein at each concentration to mAb HK44 or HK24 are depicted as a sigmoidal dose response curve in **Fig. 4 C and 4D**. These results clearly illustrate the higher specific affinity of the mAbs HK44 and HK24 for the E2 protein.

Identification of the binding of the mAbs HK24 and HK44 to a conserved epitope on the CSFV E2 protein based on a 3D structural model

To obtain detailed structural information on E2-mAbs interactions, protein-protein docking was performed. Before docking, the best protein modelling result was selected based on the probability density function (PDF) total energy and discrete optimized protein energy (DOPE). The PDF total energy and DOPE of HK24, HK44 and the E2 protein were 2296.5857, -45243.882812; 2390.8101, -46726.902344; and 1949.7089, -28135.984375, respectively. Furthermore, there were fewer irrational amino acid residues in the Ramachandran Plot, suggesting that the models we built may exist. Thus, protein-protein docking was performed by setting the Fab as the receptor protein and the E2 as the ligand protein. The docking results of E2-HK24 and E2-HK44 are shown in (**Fig. 5A and 5B)**. More precisely, we found that the epitope Cys141-Lys155 of the E2 motif in both cases was buried in the middle of V_L-V_H interface of the E2-HK24 or E2-HK44 protein complex, and this epitope contacted the Fab CDR H3, CDR L3 and CDR L1 loops in both structures in addition to CDR H2 in the HK44-E2 complex (**Fig. 5C and 5D**). In addition, the mAb HK44 also directly bind to Thr88 and Pro90 (a linear epitope on E2 protein spanning Leu84-Pro90 residues that has been reported) (26, 27) by means of three residues (Val111A, Ser111B and Tyr111C) on the tip of the loop which is a relatively long CDR H3 loop (21 amino acids) (**Fig. 5C**). As shown in **Fig. 5D**, similar to E2-HK44 protein complex, the long CDR H3 of mAb HK24 (17 amino acids) not only binds to the epitope-76, but also binds to the linear epitope on E2 protein spanning Leu84-Pro90, via some hydrogen bonds and hydrophobic interaction. Detailed interactions between antigen and antibodies are shown in the **Table 2 and 3**.

To further confirm the interaction between mAb HK44 or HK24 and epitope-76, Virtual Alanine Mutation Scanning (VAMS) was employed to calculate mutation energy of individual amino acid residues changes using Discovery Studio 2017. In the case of E2-HK44 complex, when the residues of epitope-76 of E2 protein were individually mutated to alanine, seven residues on epitope-76, namely, Val144, Ser145, Pro146, Thr147, Arg150, Glu152, Val154 generated the mutation energy higher than 0.5 kcal/mol, indicating an unstable protein complex **(Fig. 5E)**. The mutations of epitope-76 in the E2-HK24 complex procedure also destabilize the protein complex **(Fig. 5F)**. When we mutate all of the epitopes to alanine, the mutation energy is 3.63 kcal/mol for E2-HK24 protein complex and 7.28 kcal/mol for E2-HK44 protein complex, indicating that the protein complex is an unstable state. In summary, these results suggested that the mAb HK24 or HK44 binds to the E2 protein by the recognition of the epitope-76 (CTAVSPTTLRTEVV).

MAbs HK24 and HK44 can significantly neutralize CSFV *in vitro*

We next evaluated the protective efficacy of the mAbs HK24 and K44 against CSFV infection in PK-15 cells. A neutralization test was first performed via indirect immunofluorescence assay (IFA). As shown in **Fig. 6A**, the mAbs HK24 and HK44 displayed

bioRxiv preprint doi: https://doi.org/10.1101/389361; this version posted August 10, 2018. The copyright holder for this preprint (which was not certified by peer review) is the author/funder, who has granted bioRxiv a license to display the preprint in perpetuity. It is made available under aCC-BY-NC-ND 4.0 International license.

high neutralizing activity against CSFV, as no fluorescence was observed at the concentration of 75 μg/ml, and only weak fluorescence signals were detected at the concentration of 1.1 μg/ml, which was same as that observed for CSFV-positive serum. In contrast, strong fluorescence signals were detected in cells treated with CSFV-negative serum, indicating no inhibition of CSFV infection. The range of 50% inhibitory concentrations (IC_{50}) to the non-neutralizing concentration for mAbs HK24 and HK44 is presented in **Fig. 6B**. These results indicated that the mAbs HK24 and HK44 exhibited neutralizing activity against CSFV, and they can prevent CSFV infections in cells.

To further directly detect whether the mAbs HK24 and HK44 block CSFV infection, the copy numbers of CSFV RNA in PK-15 cells were analysed via qRT-PCR with specific primers. The results suggested that treating PK-15 cells with the HK44-CSFV or HK24-CSFV complex at concentrations of 75 μg/ml to 1.1 μg/ml resulted in obviously lower numbers of virus copies in the cells than those observed with negative control treatment; at the same time, the mAb HK44 showed better neutralization activity than the mAb HK24 (**Fig. 6C and 6D**).

In summary, these data indicated that the mAbs HK24 and HK44 significantly neutralized CSFV and played an essential role in preventing CSFV from infecting target cells.

Discussion

CSF is a disease that threatens the pork industry and has caused tremendous economic losses. As an alternative, development of effective vaccines and therapeutics agents may be a direct and effective approach to minimizing these losses. With the technological advances, mAbs now represent an important class of biotherapeutics, which can be used to treat autoimmune disorders diseases, cancer and viral or bacterial infections (28). Thus, it is necessary to establish a simple, highly efficient, low-cost method to produce anti-CSFV NAbs.

For generation of human mAbs, there have been previous reports of approaches involving the sorting of single B cells via FACS using fluorescently-labelled specific membrane immunoglobulins as antigen bait; However, this method may be limited by the number of antigenic baiting reagents (29-31). Here, we describe a method for efficient production of mAbs from immunized swine. We used a fluoresceinated linear neutralizing epitope CTAVSPTTLRTEVVK and FITC-labelled goat anti-pig IgG as bait for flow cytometry to screen B cells from a pig that had been pre-screened for high-level CSFV-specific antibody response in the blood. The cognate immunoglobulin heavy- and light-chain genes were then isolated from epitope-specific single B cells using single-cell RT-PCR technology. The key features of this method are the (a) sorting of B cells using a specific linear epitope by FACS, which may avoid the limitation of the availability of multiple antigenic baiting reagents; (b) direct isolation of natively matched full-length heavy- and light-chain pairs from a single B cell, thus, producing natural mAbs with a lower the risk of immunogenicity *in vivo* and greater suitability for *in vivo* applications; (c) rescue of mAbs that recognize the specific linear epitope. In contrast to traditional methods for generating mAbs, such as hybridoma technology, Epstein-Barr virus-transformation and phage-display libraries, this method helps to improve the recovery efficiency of mAbs as 78% of the mAbs

bioRxiv preprint doi: https://doi.org/10.1101/389361; this version posted August 10, 2018. The copyright holder for this preprint (which was not certified by peer review) is the author/funder, who has granted bioRxiv a license to display the preprint in perpetuity. It is made available under aCC-BY-NC-ND 4.0 International license.

produced showed neutralizing activity against CSFV. Taken together, this method is more convenient and efficient for obtaining epitope-specific NAbs against CSFV.

In this study, we amplified full-length heavy- and light-chain genes from one hundred single B cells and obtained nine mAbs, among which three were identical to HK24 and four to HK44. Thus, two mAbs HK24 and HK44 were selected to detect the strong binding reactivity against CSFV via Western blotting. To further define their binding paratopes, we tested the reactivity of the mAbs HK24 and HK44 with recombinant E2 via indirect ELISA and SPR. The results showed that the mAbs HK24 and HK44 exhibited comparable reactivity to the E2 protein. The binding sites within the linear epitope CTAVSPTTLRTEVVK on the E2 protein surface were predicted through a 3D structural model. Notably, these results are consistent with reports that the linear epitope CTAVSPTTLRTEVVK on the E2 protein is specifically recognized by CSFV antibodies (23, 32). Because the linear epitope is conserved in diverse CSFV strains and is divergent in the BVDV and BDV strains, we deduced that the mAbs HK44 and HK24 might be applied for the development of diagnostic reagents for CSFV.

We also confirmed that the mAbs HK24 and HK44 exhibited a powerful neutralizing response against the CSFV Shimen strain *in vitro*; in particular, the mAb HK44 showed an $IC_{50} \leq 1.1$ μg/ml (**Fig. 6B**). This result indicated that these mAbs are capable of blocking virus infection and provided implications for therapeutic designs. Moreover, neutralization assays showed that in this work, the mAb HK44 exhibited more excellent neutralizing activity than the mAb HK24. We deduced that this may be due to a longer CDR H3 (21 amino acids) because the amino acid lengths of the predominant CDR H3 are conserved in most vertebrates, averaging 12-16 amino acids (33). Indeed, some longer CDR H3 loops usually play an important role in the adaptive immune response such as virus neutralization as described previously (34-36). Elongated CDR H3 can better overcome the structural barriers presented by antigens to confer protective functions.

In conclusion, this is the first report to describe the isolation of whole-porcine NAbs against the E2 protein of CSFV from single B cells of a vaccinated pig using a specific linear epitope. In this study, we characterized the functions of the mAbs HK24 and HK44 through a panel of assays. The results demonstrated that HK24 and HK44 displayed high sensitivity to CSFV, indicating that these mAbs have great potential for the detection and treatment of viral infections. In addition, we established a simple and rapid method for the isolation of specific B cells. The mAbs that we generated were derived directly from porcine B cells and are therefore safer and more efficient than mAbs produced in mice, rabbits or other species.

Materials and methods

Cell lines and virus

PK-15 cells (porcine kidney cell line, ATCC, CCL-33) and HEK293T cells (human embryonic kidney cell line, ATCC, Manassas, VA) were cultured in Dulbecco's minimal essential medium (DMEM, Gibco, America) supplemented with 10% heat-inactivated foetal bovine serum (FBS, Gibco, America), at 37 ℃ in 5% CO_2. CSFV (strain Shimen) was gifts from Dr. Changchun Tu (Academy of Military Medical Sciences, Changchun, China).

Single B cell sorting

bioRxiv preprint doi: https://doi.org/10.1101/389361; this version posted August 10, 2018. The copyright holder for this preprint (which was not certified by peer review) is the author/funder, who has granted bioRxiv a license to display the preprint in perpetuity. It is made available under aCC-BY-NC-ND 4.0 International license.

Blood samples were isolated from a swine with a high-level CSFV-specific antibody response that received primary immunization with an attenuated vaccine strain of CSFV and subsequent boosting two times at one-week intervals with the same vaccine. Peripheral blood mononuclear cells (PBMCs) were isolated and suspended in phosphate-buffered saline (PBS). cells were stained for 30 min at 4 ℃ using FITC-labelled goat anti-pig IgG (Sigma-Aldrich, USA) and 5-TAMRA-conjugated epitope-76, which is a conserved epitope (CTAVSPTTLRTEVVK) on the E2 protein of CSFV (synthesized by China Peptides Co., Ltd., China) (37). All buffers used for staining contained 2% FBS (vol/vol) to block non-specific binding. Single cells were sorted via flow cytometry into 0.2-ml thin-walled PCR tubes containing 20 μl of cell lysis buffer supplemented with 1 μl of RNase inhibitor, 19 μl of 0.2% (vol/vol) Triton X-100 (Sigma-Aldrich, USA), 1 μl of oligo-dT primer and 1 μl of dNTP mix. The cells were stored at -80 ℃ until use (38, 39).

Isolation and expression of Ig gene

PCR was performed to amplify the full-length immunoglobulin heavy- and light-chain genes (*IgH* and *IgL*) from single B cells as described previously (40, 41). Briefly, to obtain Ig genes, we performed a reverse transcription reaction using SuperScript II reverse transcriptase (38, 42). Next, the *IgH, Igλ* and *Igκ* genes were amplified separately via nested PCR reactions using a mixture of primers that were specific for heavy chain, kappa light chain and lambda light chain; all oligonucleotide primers are listed in **Table 1**. The PCR products of the full-length heavy- and light-chain genes were confirmed via sequencing and were separately cloned into the pEGFP-C1 expression vector with the EF1α promoter and WPRE element (**Fig. S1**). To produce mAbs, plasmids encoding immunoglobulin heavy- and light-chains were transiently co-transfected into HEK293T cells using PowerTrans293 Transfection Reagent (Throne Science, Shanghai, China) following the manufacturer's instructions. After culturing for four days at 37 ℃ under 5% CO_2 in 6-well plates, supernatants were harvested via centrifugation, and antibodies were purified using Protein A (GenScript, USA Inc.) and quantified using a NanoDrop 2000.

SDS-polyacrylamide gel electrophoresis (SDS-PAGE) and Western blotting analysis

SDS-PAGE was performed as follows. Briefly, antibody samples were separated in 12% (reducing conditions) resolving gels and 4% stacking gels, and protein bands were stained using Coomassie brilliant blue R-250 (43). For Western blotting analysis, we collected CSFV-infected cells and uninfected cells separately in cold PBS and lysed them using a lysis buffer (Beyotime, China) that contained 1 mM phenylmethylsulfonyl fluoride (PMSF) for 5 min on ice. After centrifugation at 10,000 × g at 4 ℃ for 10 min, the supernatants were harvested and transferred into new 1.5-ml centrifuge tubes (44). Protein concentrations were determined with an enhanced-bicinchoninic acid (BCA) protein assay kit (Beyotime, China).

Western blotting was performed according to a previously described procedure (45). Briefly, equal amounts of proteins were loaded on a 12% SDS-PAGE gel. Next, the separated proteins were transferred onto nitrocellulose membranes, which were blocked with 5% (wt/vol) non-fat milk in Tris-buffered saline that contained 0.2-0.4% Tween-20 (TBS-T) for 2 h at room temperature. The membranes were probed with 4 μg/ml mAb or porcine IgGs (hyperimmune serum). Next, the bound antibody was stained using 2 μg/ml horseradish

bioRxiv preprint doi: https://doi.org/10.1101/389361; this version posted August 10, 2018. The copyright holder for this preprint (which was not certified by peer review) is the author/funder, who has granted bioRxiv a license to display the preprint in perpetuity. It is made available under aCC-BY-NC-ND 4.0 International license.

peroxidase (HRP)-conjugated rabbit anti-pig antibodies (Beijing Biosynthesis Biotechnology Co. Ltd, China). Immunoreactive bands were visualized using the ECL detection reagent (Beyotime, China) and the Azure c600 Western blot imaging system.

Immunofluorescence to detect the binding specificity of mAbs HK44 and HK24 to epitope-76

The binding of epitope-76 to mAbs HK44 and HK24 were determined via immunofluorescence. In this procedure, enzyme-linked immunosorbent assay (ELISA) plates were coated with 100 µl (2 µg/ml) of a positive polyclonal antibody, mAbs HK24 and HK44 diluted in carbonate bicarbonate buffer (pH 9.6) and were incubated at 4 ℃ overnight (46). The next day, the plates were washed thrice with PBS containing 0.05% Tween-20 (PBS-T), and 100 µl of blocking buffer (5% non-fat dry milk in PBS) was added per well. The plates were incubated at 37 ℃ for 1 h. After blocking, 100 µl of FITC-conjugated epitope-76 or unrelated FITC-conjugated epitope-75 was added into each well, and the plates were incubated at 37 ℃ for 2 h. Finally, fluorescence intensity was measured using a Tecan Microplate reader.

Expression of the E2 protein

The partial sequence of E2 gene (GenBank: AY775178.2) was amplified from CSFV-infected cell mRNA via PCR and cloned into an expression vector (47). The vector was transformed into *E. coli* Rosetta (DE3) cells, and the transformants were selected and cultured in LB. The overnight cultures were subcultured at 1:100 and grown to an OD_{600} of 0.6 at 37 ℃. Next, 0.1 mM isopropyl-b-D-thiogalactopyranoside (IPTG) was added to induce the expression of the protein at 25 ℃ for 12 h. The induced culture was harvested via centrifugation at 6,500 × g for 15 min at 4 ℃ and sonicated on ice. Subsequently, the inclusion bodies were separated from the crude cell lysate via centrifugation at 10,000 × g for 10 min and dissolved in 6 M urea at room temperature for 6 h. Finally, soluble E2 protein was purified through Ni-NTA resin as described previously (48, 49).

Detecting the affinity of mAbs HK24 and HK44 for the CSFV E2 protein via indirect ELISA

An indirect ELISA was used to determine the affinity of the mAbs for the CSFV E2 protein. Purified E2 protein (2 µg/ml) was used to coat ELISA plates at 4 ℃ overnight. The next day, the plates were washed thrice with PBS-T, and 100 µl of blocking buffer (5% nonfat dry milk in PBS) was added per well. The plates were incubated at 37 ℃ for 1 h. After blocking, 100 µl of antibody samples were added per well, and the plates were incubated at 37 ℃ for 2 h. Thereafter, an HRP-conjugated rabbit anti-pig antibody (Beijing Biosynthesis Biotechnology Co. Ltd, China) was added into each well at 37 ℃ for 1 h. Finally, the wells were washed and incubated with 100 µl of TMB/H_2O_2 substrate per well at room temperature for 10 min. The reaction was stopped using 50 µl of 2 M H_2SO_4 per well, and the absorbance was read at 450 nm.

Modelling of the E2 protein and the antigen-binding (Fab) fragment of the mAbs HK24 and HK44

bioRxiv preprint doi: https://doi.org/10.1101/389361; this version posted August 10, 2018. The copyright holder for this preprint (which was not certified by peer review) is the author/funder, who has granted bioRxiv a license to display the preprint in perpetuity. It is made available under aCC-BY-NC-ND 4.0 International license.

The interactions of mAbs HK24 and HK44 with the CSFV E2 protein were simulated using Discovery Studio 2017. To obtain a three-dimensional model of the mAb HK24, we searched for a similar sequence in the Protein Data Bank (PDB) database. We found that the sequence homology between an anti-G-quadruplex-containing RNA antibody crystal (PDB 4KZD) and Fab of HK24 consisted of 84.1% similarity and 72.7% identity. Therefore, we used PDB 4KZD as a template for modelling the mAb HK24 Fab. Considering the quality of mAb HK44 model, we selected a chimeric template for modelling. For this purpose, humanized antibody 4B12 Fab (PDB 4LKX), an anti-TDRD3 FAB (PDB 3PNW) and an anti-CMV Fab Fragment (PDB 4LRI) were used as templates for modelling the light chain (LC), heavy chain (HC) and the interface of the mAb HK44 Fab; the sequence homologies (similarity and identity) between each template and the mAb HK44 Fab were 87.7% and 74.9% for V_L, 80.4% and 70.9% for V_H and 82.8% and 69.8% for the entire Fab, respectively. E2 protein modelling was performed using the template of the crystal of the BVDV1 envelope glycoprotein E2 (PDB 2YQ2, 60% sequence identity with E2) (50).

Docking and analysis of protein complexes

Before docking, models were typed using the CHARMm Polar H forcefield. We set E2 as the ligand protein and the Fab of HK24/HK44 as the receptor protein. ZDOCK, a rigid-body protein-protein docking algorithm based on the Fast Fourier Transform Correlation technique, was used with a 6° angular step size to generate 54,000 poses, of which the top 2000 were re-ranked by ZRANK (51). These poses were then processed with RDOCK, and only the top 10 clusters with the highest density of poses were further considered. Finally, we used the "Analyze Protein Interface" protocol for analysis. All docking calculations were performed using Discovery Studio 2017.

Surface plasmon resonance (SPR) analysis

To analyse the affinity of the mAbs for the CSFV E2 protein, we performed SPR analysis on a Biacore 8K system (GE Healthcare) using CM5 sensor chips (GE Healthcare) and PBS-T as the running buffer during immobilization and binding analysis at a constant temperature of 25℃ (52). Initially, the surface was activated with 1-ethyl-3-(3-dimethylaminopropyl)-carbodiimide (EDC) and N-hydroxysuccinimide (NHS), and the mAb HK44 or HK24 was diluted in 10 mM sodium acetate buffer (pH 4.0) and immobilized on the CM5 sensor chip using Amine Coupling Kit (GE Healthcare). Next, for binding analysis, five different concentrations of the recombinant E2 protein diluted in the running buffer (2000 nM, 1000 nM, 500 nM, 250 nM, and 125 nM) were allowed to flow over the chip surface. After sample injection was completed, the running buffer was allowed to flow over the surface to perform dissociation. At the end of dissociation, the sensor surface was regenerated with a glycine-HCl solution (53). Finally, all experimental data were analysed using Biacore 8K evaluation software (GE Healthcare).

Neutralization assays

The neutralization activity of the mAbs HK24 and HK44 against CSFV was tested via an immunofluorescence assay as described previously (54). Briefly, PK-15 cells were grown to 30-40% confluence in complete DMEM containing 10% FBS on 96-well plates at 37℃ in 5%

bioRxiv preprint doi: https://doi.org/10.1101/389361; this version posted August 10, 2018. The copyright holder for this preprint (which was not certified by peer review) is the author/funder, who has granted bioRxiv a license to display the preprint in perpetuity. It is made available under aCC-BY-NC-ND 4.0 International license.

446 CO_2. Antibodies (150 μg/ml) were diluted two-fold in DMEM in a series and mixed 1:1 with
447 100 $TCID_{50}$ CSFV, and the mixtures were incubated at 37 ℃ for 1 h. After incubation, 100 μl
448 of the antibody-virus mixture was added into the wells of the 96-well plates to infect the
449 PK-15 cells for 2 h. Uninfected cells and virus-infected cells acted as positive and negative
450 controls, respectively. After 2 h of incubation, the supernatants were aspirated, and the cells
451 were washed three times with PBS. Next, 200 μl of fresh medium was added, and the cells
452 were incubated at 37 ℃ for 72 h. Subsequently, the cells were fixed with 80% cold acetone at
453 -20 ℃ overnight. The next day, the cells were washed and incubated with porcine
454 CSFV-positive serum (1:100 dilution in PBS containing 10% FBS) at 37 ℃ for 2 h. After
455 being washed three times with PBS, FITC-labelled goat anti-pig IgG (Sigma-Aldrich,
456 America) was added into each well, and the plates were incubated at 37 ℃ for 0.5 h (55).
457 Images were obtained using fluorescence microscopy (Olympus BX51).
458
459 **Quantification of CSFV RNA**
460 Quantitative RT-PCR (qRT-PCR) was performed to examine CSFV in PK-15 cells. Total
461 RNA was extracted from the uninfected and virus-infected cells using TRIzol (Tiangen,
462 Beijing, China), according to the manufacturer's instructions. Reverse transcription reactions
463 were performed using the FastKing RT Kit (Tiangen, Beijing, China) to synthetize cDNA, and
464 qRT-PCR was performed on a Bio-RadiQ5 instrument (BioRad, USA) with SuperReal
465 PreMix Plus (Tiangen, Beijing, China). A standard curve was simultaneously created to
466 calculate the viral load in each sample.
467
468 **Statistical analysis**
469 All data presented in the figures are expressed as the mean ± SD from at least three
470 independent experiments. When the data from the neutralization assays were analysed, the
471 antibody concentrations were transformed to $\log_{10}$, and the IC_{50} was calculated using
472 GraphPad Prism software 7.0 (La Jolla, CA, America) with the equation for dose response
473 (variable slope). $P < 0.05$ was considered statistically significant.
474
475 **Acknowledgements**
476 We would like to thank Xue Chen for technical assistance. This study was financially
477 supported by a grant from the Special Funds for Cultivation and Breeding of New Transgenic
478 Organisms (No. 2016ZX08006003), the Program for JLU Science and Technology Innovative
479 Research Team (2017TD-28), the Program for Changjiang Scholars and Innovative Research
480 Team in University in China (No. IRT16R32), the Fundamental Research Funds for the
481 central Universities, the Jilin Province Science and Technology Development Projects (No.
482 20150204077NY) and the National Natural Science Foundation of China (No. 31772747).
483
484 **Conflict of Interest**
485 The authors declare that they have no competing interests.
486
487 **Ethical Approval**
488 Not applicable.
489

bioRxiv preprint doi: https://doi.org/10.1101/389361; this version posted August 10, 2018. The copyright holder for this preprint (which was not certified by peer review) is the author/funder, who has granted bioRxiv a license to display the preprint in perpetuity. It is made available under aCC-BY-NC-ND 4.0 International license.

References

1. **Tamura T, Nagashima N, Ruggli N, Summerfield A, Kida H, Sakoda Y.** 2014. Npro of classical swine fever virus contributes to pathogenicity in pigs by preventing type I interferon induction at local replication sites. Veterinary research **45:**47.
2. **Lamp B, Riedel C, Roman-Sosa G, Heimann M, Jacobi S, Becher P, Thiel HJ, Rumenapf T.** 2011. Biosynthesis of classical swine fever virus nonstructural proteins. J Virol **85:**3607-3620.
3. **Chandriani S, Skewes-Cox P, Zhong W, Ganem DE, Divers TJ, Van Blaricum AJ, Tennant BC, Kistler AL.** 2013. Identification of a previously undescribed divergent virus from the Flaviviridae family in an outbreak of equine serum hepatitis. Proceedings of the National Academy of Sciences of the United States of America **110:**E1407-1415.
4. **Becher P, Avalos Ramirez R, Orlich M, Cedillo Rosales S, König M, Schweizer M, Stalder H, Schirrmeier H, Thiel H-J.** 2003. Genetic and antigenic characterization of novel pestivirus genotypes: implications for classification. Virology **311:**96-104.
5. **Meyers G, Thiel HJ.** 1996. Molecular characterization of pestiviruses. Advances in virus research **47:**53-118.
6. **Wang Z, Nie Y, Wang P, Ding M, Deng H.** 2004. Characterization of classical swine fever virus entry by using pseudotyped viruses: E1 and E2 are sufficient to mediate viral entry. Virology **330:**332-341.
7. **Risatti GR, Borca MV, Kutish GF, Lu Z, Holinka LG, French RA, Tulman ER, Rock DL.** 2005. The E2 glycoprotein of classical swine fever virus is a virulence determinant in swine. J Virol **79:**3787-3796.
8. **Edwards S, Sands JJ.** 1990. Antigenic comparisons of hog cholera virus isolates from Europe, America and Asia using monoclonal antibodies. DTW. Deutsche tierarztliche Wochenschrift **97:**79-81.
9. **Yu M, Wang LF, Shiell BJ, Morrissy CJ, Westbury HA.** 1996. Fine mapping of a C-terminal linear epitope highly conserved among the major envelope glycoprotein E2 (gp51 to gp54) of different pestiviruses. Virology **222:**289-292.
10. **Burton DR, Hangartner L.** 2016. Broadly Neutralizing Antibodies to HIV and Their Role in Vaccine Design. Annu Rev Immunol **34:**635-659.
11. **Pasqualini R, Arap W.** 2004. Hybridoma-free generation of monoclonal antibodies. Proceedings of the National Academy of Sciences of the United States of America **101:**257-259.
12. **Cole SP, Campling BG, Atlaw T, Kozbor D, Roder JC.** 1984. Human monoclonal antibodies. Molecular and cellular biochemistry **62:**109-120.
13. **Reichert JM, Rosensweig CJ, Faden LB, Dewitz MC.** 2005. Monoclonal antibody successes in the clinic. Nature biotechnology **23:**1073-1078.
14. **Kohler G, Milstein C.** 2005. Continuous cultures of fused cells secreting antibody of predefined specificity. 1975. Journal of immunology **174:**2453-2455.
15. **Burton DR, Barbas CF, 3rd, Persson MA, Koenig S, Chanock RM, Lerner RA.** 1991. A large array of human monoclonal antibodies to type 1 human immunodeficiency virus from combinatorial libraries of asymptomatic seropositive individuals. Proceedings of the National Academy of Sciences of the United States of America **88:**10134-10137.
16. **Wilson PC, Andrews SF.** 2012. Tools to therapeutically harness the human antibody response. Nature reviews. Immunology **12:**709-719.
17. **Sun Z, Yan L, Tang J, Qian Q, Lenberg J, Zhu D, Liu W, Wu K, Wang Y, Lu S.** 2018. Brief introduction of current technologies in isolation of broadly neutralizing HIV-1 antibodies. Virus Res **243:**75-82.
18. **Bornholdt ZA, Turner HL, Murin CD, Li W, Sok D, Souders CA, Piper AE, Goff A, Shamblin JD, Wollen SE, Sprague TR, Fusco ML, Pommert KBJ, Cavacini LA, Smith HL, Klempner M, Reimann KA, Krauland**

bioRxiv preprint doi: https://doi.org/10.1101/389361; this version posted August 10, 2018. The copyright holder for this preprint (which was not certified by peer review) is the author/funder, who has granted bioRxiv a license to display the preprint in perpetuity. It is made available under aCC-BY-NC-ND 4.0 International license.

E, Gerngross TU, Wittrup KD, Saphire EO, Burton DR, Glass PJ, Ward AB, Walker LM. 2016. Isolation of potent neutralizing antibodies from a survivor of the 2014 Ebola virus outbreak. Science **351:**1078-1083.

19. **Sok D, Le KM, Vadnais M, Saye-Francisco KL, Jardine JG, Torres JL, Berndsen ZT, Kong L, Stanfield R, Ruiz J, Ramos A, Liang CH, Chen PL, Criscitiello MF, Mwangi W, Wilson IA, Ward AB, Smider VV, Burton DR.** 2017. Rapid elicitation of broadly neutralizing antibodies to HIV by immunization in cows. Nature **548:**108-111.

20. **Robbiani DF, Bozzacco L, Keeffe JR, Khouri R, Olsen PC, Gazumyan A, Schaefer-Babajew D, Avila-Rios S, Nogueira L, Patel R, Azzopardi SA, Uhl LFK, Saeed M, Sevilla-Reyes EE, Agudelo M, Yao KH, Golijanin J, Gristick HB, Lee YE, Hurley A, Caskey M, Pai J, Oliveira T, Wunder EA, Jr., Sacramento G, Nery N, Jr., Orge C, Costa F, Reis MG, Thomas NM, Eisenreich T, Weinberger DM, de Almeida ARP, West AP, Jr., Rice CM, Bjorkman PJ, Reyes-Teran G, Ko AI, MacDonald MR, Nussenzweig MC.** 2017. Recurrent Potent Human Neutralizing Antibodies to Zika Virus in Brazil and Mexico. Cell **169:**597-609 e511.

21. **Labrijn AF, Poignard P, Raja A, Zwick MB, Delgado K, Franti M, Binley J, Vivona V, Grundner C, Huang CC, Venturi M, Petropoulos CJ, Wrin T, Dimitrov DS, Robinson J, Kwong PD, Wyatt RT, Sodroski J, Burton DR.** 2003. Access of antibody molecules to the conserved coreceptor binding site on glycoprotein gp120 is sterically restricted on primary human immunodeficiency virus type 1. J Virol **77:**10557-10565.

22. **Chen SC, Li S, Sun HM, Li YF, Ji SW, Song K, Zhang LK, Luo YZ, Sun Y, Ma JF, Liu PH, Qiu HJ.** 2018. Expression and characterization of a recombinant porcinized antibody against the E2 protein of classical swine fever virus. Appl Microbiol Biot **102:**961-970.

23. **Qi Y, Liu LC, Zhang BQ, Shen Z, Wang J, Chen YH.** 2008. Characterization of antibody responses against a neutralizing epitope on the glycoprotein E2 of classical swine fever virus. Arch Virol **153:**1593-1598.

24. **Viitala T, Granqvist N, Hallila S, Ravina M, Yliperttula M.** 2013. Elucidating the Signal Responses of Multi-Parametric Surface Plasmon Resonance Living Cell Sensing: A Comparison between Optical Modeling and Drug-MDCKII Cell Interaction Measurements. PloS one **8**.

25. **De Crescenzo G, Boucher C, Durocher Y, Jolicoeur M.** 2008. Kinetic Characterization by Surface Plasmon Resonance-Based Biosensors: Principle and Emerging Trends. Cell Mol Bioeng **1:**204-215.

26. **Peng WP, Hou Q, Xia ZH, Chen D, Li N, Sun Y, Qiu HJ.** 2008. Identification of a conserved linear B-cell epitope at the N-terminus of the E2 glycoprotein of Classical swine fever virus by phage-displayed random peptide library. Virus Res **135:**267-272.

27. **El Omari K, Iourin O, Harlos K, Grimes JM, Stuart DI.** 2013. Structure of a Pestivirus Envelope Glycoprotein E2 Clarifies Its Role in Cell Entry. Cell reports **3:**30-35.

28. **Chadd HE, Chamow SM.** 2001. Therapeutic antibody expression technology. Curr Opin Biotech **12:**188-194.

29. **Magnani DM, Rogers TF, Beutler N, Ricciardi MJ, Bailey VK, Gonzalez-Nieto L, Briney B, Sok D, Le K, Strubel A, Gutman MJ, Pedreno-Lopez N, Grubaugh ND, Silveira CGT, Maxwell HS, Domingues A, Martins MA, Lee DE, Okwuazi EE, Jean S, Strobert EA, Chahroudi A, Silvestri G, Vanderford TH, Kallas EG, Desrosiers RC, Bonaldo MC, Whitehead SS, Burton DR, Watkins DI.** 2017. Neutralizing human monoclonal antibodies prevent Zika virus infection in macaques. Sci Transl Med **9**.

30. **Huang J, Doria-Rose NA, Longo NS, Laub L, Lin CL, Turk E, Kang BH, Migueles SA, Bailer RT, Mascola JR, Connors M.** 2013. Isolation of human monoclonal antibodies from peripheral blood B cells. Nature protocols **8:**1907-1915.

bioRxiv preprint doi: https://doi.org/10.1101/389361; this version posted August 10, 2018. The copyright holder for this preprint (which was not certified by peer review) is the author/funder, who has granted bioRxiv a license to display the preprint in perpetuity. It is made available under aCC-BY-NC-ND 4.0 International license.

31. **Wardemann H, Yurasov S, Schaefer A, Young JW, Meffre E, Nussenzweig MC.** 2003. Predominant autoantibody production by early human B cell precursors. Science **301:**1374-1377.

32. **van der Wal FJ, Jelsma T, Fijten H, Achterberg RP, Loeffen WL.** 2016. Towards a peptide-based suspension array for the detection of pestivirus antibodies in swine. Journal of virological methods **235:**15-20.

33. **Wang F, Ekiert DC, Ahmad I, Yu W, Zhang Y, Bazirgan O, Torkamani A, Raudsepp T, Mwangi W, Criscitiello MF, Wilson IA, Schultz PG, Smider VV.** 2013. Reshaping antibody diversity. Cell **153:**1379-1393.

34. **Collis AVJ, Brouwer AP, Martin ACR.** 2003. Analysis of the Antigen Combining Site: Correlations Between Length and Sequence Composition of the Hypervariable Loops and the Nature of the Antigen. Journal of molecular biology **325:**337-354.

35. **Kodangattil S, Huard C, Ross C, Li J, Gao H, Mascioni A, Hodawadekar S, Naik S, Min-debartolo J, Visintin A, Almagro JC.** 2014. The functional repertoire of rabbit antibodies and antibody discovery via next-generation sequencing. mAbs **6:**628-636.

36. **Pejchal R, Walker LM, Stanfield RL, Phogat SK, Koff WC, Poignard P, Burton DR, Wilson IA.** 2010. Structure and function of broadly reactive antibody PG16 reveal an H3 subdomain that mediates potent neutralization of HIV-1. Proceedings of the National Academy of Sciences of the United States of America **107:**11483-11488.

37. **Carbonetti S, Oliver BG, Vigdorovich V, Dambrauskas N, Sack B, Bergl E, Kappe SHI, Sather DN.** 2017. A method for the isolation and characterization of functional murine monoclonal antibodies by single B cell cloning. Journal of immunological methods **448:**66-73.

38. **Picelli S, Faridani OR, Bjorklund AK, Winberg G, Sagasser S, Sandberg R.** 2014. Full-length RNA-seq from single cells using Smart-seq2. Nature protocols **9:**171-181.

39. **Bornholdt ZA, Turner HL, Murin CD, Li W, Sok D, Souders CA, Piper AE, Goff A, Shamblin JD, Wollen SE, Sprague TR, Fusco ML, Pommert KB, Cavacini LA, Smith HL, Klempner M, Reimann KA, Krauland E, Gerngross TU, Wittrup KD, Saphire EO, Burton DR, Glass PJ, Ward AB, Walker LM.** 2016. Isolation of potent neutralizing antibodies from a survivor of the 2014 Ebola virus outbreak. Science **351:**1078-1083.

40. **Tiller T, Meffre E, Yurasov S, Tsuiji M, Nussenzweig MC, Wardemann H.** 2008. Efficient generation of monoclonal antibodies from single human B cells by single cell RT-PCR and expression vector cloning. Journal of immunological methods **329:**112-124.

41. **Liao HX, Bonsignori M, Alam SM, McLellan JS, Tomaras GD, Moody MA, Kozink DM, Hwang KK, Chen X, Tsao CY, Liu PH, Lu XZ, Parks RJ, Montefiori DC, Ferrari G, Pollara J, Rao M, Peachman KK, Santra S, Letvin NL, Karasavvas N, Yang ZY, Dai KF, Pancera M, Gorman J, Wiehe K, Nicely NI, Rerks-Ngarm S, Nitayaphan S, Kaewkungwal J, Pitisuttithum P, Tartaglia J, Sinangil F, Kim JH, Michael NL, Kepler TB, Kwong PD, Mascola JR, Nabel GJ, Pinter A, Zolla-Pazner S, Haynes BF.** 2013. Vaccine Induction of Antibodies against a Structurally Heterogeneous Site of Immune Pressure within HIV-1 Envelope Protein Variable Regions 1 and 2. Immunity **38:**176-186.

42. **Picelli S, Bjorklund AK, Faridani OR, Sagasser S, Winberg G, Sandberg R.** 2013. Smart-seq2 for sensitive full-length transcriptome profiling in single cells. Nature methods **10:**1096-1098.

43. **Giritch A, Marillonnet S, Engler C, van Eldik G, Botterman J, Klimyuk V, Gleba Y.** 2006. Rapid high-yield expression of full-size IgG antibodies in plants coinfected with noncompeting viral vectors. Proceedings of the National Academy of Sciences of the United States of America **103:**14701-14706.

44. **Luo L, Nishi K, Macleod E, Sabara MI, Lin M, Handel K, Pasick J.** 2013. Baculovirus expression and

bioRxiv preprint doi: https://doi.org/10.1101/389361; this version posted August 10, 2018. The copyright holder for this preprint (which was not certified by peer review) is the author/funder, who has granted bioRxiv a license to display the preprint in perpetuity. It is made available under aCC-BY-NC-ND 4.0 International license.

622 antigenic characterization of classical swine fever virus E2 proteins. Transboundary and emerging
623 diseases **60:**143-151.

624 45. **Gershoni JM, Palade GE.** 1982. Electrophoretic transfer of proteins from sodium dodecyl
625 sulfate-polyacrylamide gels to a positively charged membrane filter. Analytical biochemistry
626 **124:**396-405.

627 46. **Tarradas J, Monso M, Munoz M, Rosell R, Fraile L, Frias MT, Domingo M, Andreu D, Sobrino F, Ganges**
628 **L.** 2011. Partial protection against classical swine fever virus elicited by dendrimeric vaccine-candidate
629 peptides in domestic pigs. Vaccine **29:**4422-4429.

630 47. **Ficinska J, Szymanski P, Szewczyk B, Bienkowska-Szewczyk K.** 1999. Expression of CSFV E2
631 glycoprotein gene in baculovirus system. Med Weter **55:**677-680.

632 48. **Goto M, Hashimoto Y, Fujita T, Ono T, Furusaki S.** 2000. Important parameters affecting efficiency of
633 protein refolding by reversed micelles. Biotechnol Progr **16:**1079-1085.

634 49. **Risatti GR, Holinka LG, Carrillo C, Kutish GF, Lu Z, Tulman ER, Sainz IF, Borca MV.** 2006. Identification
635 of a novel virulence determinant within the E2 structural glycoprotein of classical swine fever virus.
636 Virology **355:**94-101.

637 50. **Grellier B, Le Pogam F, Vitorino M, Starck JP, Geist M, Duong V, Haegel H, Menguy T, Bonnefoy JY,**
638 **Marchand JB, Ancian P.** 2014. 3D modeling and characterization of the human CD115 monoclonal
639 antibody H27K15 epitope and design of a chimeric CD115 target. mAbs **6:**533-546.

640 51. **Pierce B, Weng ZP.** 2007. ZRANK: Reranking protein docking predictions with an optimized energy
641 function. Proteins **67:**1078-1086.

642 52. **Della Pia EA, Martinez KL.** 2015. Single Domain Antibodies as a Powerful Tool for High Quality Surface
643 Plasmon Resonance Studies. PloS one **10**.

644 53. **Sandomenico A, Leonardi A, Berisio R, Sanguigno L, Foca G, Foca A, Ruggiero A, Doti N, Muscariello L,**
645 **Barone D, Farina C, Owsianka A, Vitagliano L, Patel AH, Ruvo M.** 2016. Generation and
646 Characterization of Monoclonal Antibodies against a Cyclic Variant of Hepatitis C Virus E2 Epitope
647 412-422. J Virol **90:**3745-3759.

648 54. **Fu F, Li L, Shan L, Yang B, Shi H, Zhang J, Wang H, Feng L, Liu P.** 2017. A spike-specific whole-porcine
649 antibody isolated from a porcine B cell that neutralizes both genogroup 1 and 2 PEDV strains.
650 Veterinary microbiology **205:**99-105.

651 55. **Xie Z, Pang D, Wang K, Li M, Guo N, Yuan H, Li J, Zou X, Jiao H, Ouyang H, Li Z, Tang X.** 2017.
652 Optimization of a CRISPR/Cas9-mediated Knock-in Strategy at the Porcine Rosa26 Locus in Porcine
653 Foetal Fibroblasts. Sci Rep **7:**3036.

654

655

bioRxiv preprint doi: https://doi.org/10.1101/389361; this version posted August 10, 2018. The copyright holder for this preprint (which was not certified by peer review) is the author/funder, who has granted bioRxiv a license to display the preprint in perpetuity. It is made available under aCC-BY-NC-ND 4.0 International license.

Figure legends

Figure 1. Isolation of epitope-specific antibodies.

(A and B) Detection of CSFV antibodies was performed using a CSFV antibody test kit (positive blocking rate ≥ 40%, negative blocking rate ≤ 30%). (A) Blocking rate of serum samples isolated from unvaccinated pigs. (B) Blocking rate of serum samples isolated from individuals immunized with attenuated vaccine strain of CSFV. (C) Sequence alignment between E2 from four different CSFV strains, one BVDV strain and one BDV strain. The conserved amino acid residues are highlighted in red, and the somatically mutated residues are highlighted in green (BVDV stains) and blue (BDV strains). (D) Frequency of epitope-specific, IgG^+ memory B cells in the peripheral blood of pig #3748. An unvaccinated pig, #3741, was used as the negative control. Flow cytometry plots display the percentage of IgG^+ B cells that bound to FITC-conjugated epitope-76 bait. (E) List of V (D) J segments of antibody genes that we isolated and germline (GL) assignment which were derived using the international ImMunoGeneTics information system (IMGT). (F) Analysis of the expression of the mAbs HK24 and HK44 via SDS-PAGE. Samples were resolved by reducing 12% SDS-PAGE, followed by staining with Coomassie blue. Lane M, marker protein; lane 1, porcine IgGs 8 μg; lane 2, porcine IgGs 20 μg; lane 3, mAb HK24; lane 4, mAb HK44; lane 5, supernatant of control HEK293T cells. The black arrows on the right indicate the antibody heavy chains (HC) and light chains (LC).

Figure 2. Specific reactions of the mAbs HK24 and HK44 with epitope-76.

(A) Fluorescence microscopic images of cells. Green fluorescence was only observed on cells transfected with the HK24 or HK44 expression vectors. Cells transfected with empty vectors served as a negative control. Scale bar, 200 μm. (B) Analysis of the affinity of HK24 and HK44 for epitope-76. Affinity was analysed using FACS. NC is cells transfected with empty vectors. (C) Antibody specificity against epitope-76 was measured via a fluorescence assay. The mAbs HK24 and HK44 and positive IgGs isolated from pig #3748 were immobilized on an ELISA plate. Fluoresceinated epitopes were used to assess the binding activity of these antibodies. Epitope-75 is an unrelated epitope. The results from at least three biological replicates (mean ± SD) and analysed using t tests with GraphPad Prism software. $^{*}p < 0.05$, $^{**}p < 0.005$, and $^{***}p < 0.0001$.

Figure 3. The mAbs HK24 and HK44 bound to the E2 protein.

(A and B) The mAbs HK24 and HK44 bound to the CSFV E2 protein. Protein samples were obtained from PK-15 cells infected with CSFV. Uninfected PK-15 cells served as negative controls. All samples were resolved via 12% reducing SDS-PAGE and were identified using the mAbs HK24 (A) and HK44 (B). β-Actin was used as an internal control. (C) Recombinant CSFV E2 protein (690-866 aa) expressed in a bacterial system was recognized by the mAbs HK24 and HK44 and determined via Western blotting. (D) Detection of the binding of the mAbs HK24 and HK44 to the recombinant E2 protein using ELISA. Recombinant E2 protein (2 μg/ml) was used to coat the ELISA plates. The mAbs HK24 or HK44 (200 μg/ml), which were serially diluted in PBS, were added to each well. Negative IgGs were purified from CSFV-negative serum and used as a negative control. Results were obtained from at least

bioRxiv preprint doi: https://doi.org/10.1101/389361; this version posted August 10, 2018. The copyright holder for this preprint (which was not certified by peer review) is the author/funder, who has granted bioRxiv a license to display the preprint in perpetuity. It is made available under aCC-BY-NC-ND 4.0 International license.

three biological replicates (mean ± SD). (E) Detection of CSFV by the mAbs HK24 and HK44. PK-15 cells were infected with CSFV and identified via IFA using HK24, HK44, anti-CSFV swine serum and negative swine serum. Green fluorescence was observed on cells treated with HK24, HK44 and anti-CSFV swine serum. However, cells treated with negative serum showed no fluorescence. Scale bar, 200 μm.

Figure 4. SPR binding assays.

MAbs HK44 and HK24 bound to recombinant E2 protein. (A and B) Binding of E2 protein at concentrations of 2000, 1000, 500, 250 and 125 nM to mAbs (A) MAb HK44, (B) MAb HK24. The SPR data for each binding step were calculated and are shown in the table at the bottom. (C and D) Dose–response curve of the E2 binding signal. (C) The mAb HK44 binding response against each concentration of E2 protein. (D) The mAb HK24 binding response against each concentration of E2 protein.

Figure 5. 3D modelling of the combination of the Fab fragments of mAbs HK24 and HK44 with the CSFV E2 protein.

(A and B) Cartoon representation of E2-HK44 and E2-HK24 protein complex. The best docking results are displayed by the surface. Light and heavy chains of the antibody are shown in slateblue and salmon, except for the CDR loops, which are shown in cyan and violet. The E2 protein is shown in pale green, except for the epitope, which is shown in green. (A) E2-HK44 protein complex. (B) E2-HK24 protein complex. (C and D) Bonds in the interface of the protein complex. Conventional hydrogen bond is colored in green, carbon hydrogen bond is colored in cyan, electrostatic (attractive charges and Pi-Cation) is colored in orange, Alkyl Hydrophobic is colored in pink, Pi-Sigma Hydrophobic is colored in purple. (C) E2-HK44 protein complex. (D) E2-HK24 protein complex. (E and F) The value of mutation energy during Virtual Alanine Mutation on the epitope-76 in the protein-protein complex. (E) E2-HK44 protein complex. (F) E2-HK24 protein complex.

Figure 6. The mAbs HK24 and HK44 neutralize CSFV.

(A) The mAbs HK24 and HK44 were tested for neutralization reactivity with CSFV via the IFA neutralization assay. CSFV-positive serum isolated from pig #3748 served as the positive control, and CSFV-negative serum isolated from pig #3741 was used as the negative control. (B) The percentage of CSFV inhibition. The dashed line represents 50% inhibition of the virus compared to the virus-only control. (C and D) Neutralization activity of the mAbs HK24 and HK44 was measured via quantitative qRT-PCR. (C) The number of CSFV copies in cells treated with the mAb HK24. (D) The number of CSFV copies in cells treated with the mAb HK44. Results were obtained from at least three biological replicates (mean ± SD) and analyzed using t tests with GraphPad Prism software. $^{*}p < 0.05$, $^{**}p < 0.005$, and $^{***}p < 0.0001$ (versus the positive serum).

Figure S1. Physical maps of the expression vectors of the mAbs HK24 and HK44.

Plasmid pEGFP-C1 was selected as the backbone, and the CMV promoter was substituted by the EF1α promoter. (A) P24H is the expression vector of the kappa light chains of HK24. (B) P24K is the expression vector of the heavy chains of HK24. (C) P44H is the expression vector

bioRxiv preprint doi: https://doi.org/10.1101/389361; this version posted August 10, 2018. The copyright holder for this preprint (which was not certified by peer review) is the author/funder, who has granted bioRxiv a license to display the preprint in perpetuity. It is made available under aCC-BY-NC-ND 4.0 International license.

744 of the kappa light chains of HK44. (D) P44K is the expression vector of the heavy chains of
745 HK44.

746

bioRxiv preprint doi: https://doi.org/10.1101/389361; this version posted August 10, 2018. The copyright holder for this preprint (which was not certified by peer review) is the author/funder, who has granted bioRxiv a license to display the preprint in perpetuity. It is made available under aCC-BY-NC-ND 4.0 International license.

747 **TABLE 1**. Oligoes used in this study.

Oligo name	Sequences (5´-3´)	748
E2-F	CATGCCATGGCTCGGCTAGCCTGCAAGG	749
E2-R	CCGCTCGAGTAGATCTTCATTTTCCACTGTGGTGGTC	750
IGH F1	GTGTCCAGGGTGAGGAGAAGCTG	751
IGH F2	GTGTCCAGGGTCAGGAGAAGCTG	752
IGH F3	GTGTCCAGGGTGAGGTGAAGCTG	753
IGH R	CGGTGATGCACGAGGCTCTGCACAACCA	754
IGK F1	GCCATCCAGCTGACCCAGTCTCCAGCCTCC	755
IGK F2	GCCATYGTGCTGACCCAGASTCCACTCTC	756
IGK F3	GAAATTGTGCTGACCCAGTCTGCAGCC	757
IGK F4	GAAACAACAGTCACTCAATCTCCAGCAT	758
IGK R	AGCCTCACACTCGTTCCTGYTGAAGCTTTTG	759
IGL F1	TCCTATGAGGTGACTCAGCCACCCT	760
IGL F2	TCCTATGAGCTGACCCAGCCGTCTT	761
IGL F3	TCTTCTAAGCTGACTCAGCCCCCG	762
IGL F4	CAGTCTGCCCTGACTCAGCCCCCCT	763
IGL F5	TCTCAGACTGTGATCCAGGAGCCGG	764
IGL F6	TCCCTCTCCCAGGCTGTGCTGA	765
IGL F7	TCCCAGATGGTGACTCAGGAA	766
IGL F8	CCAAGCTGTGTGACTCAGGAACC	767
IGL R	GGCGCACTCGGAGGGCGTCACTGTCTT	768
IS	AAGCAGTGGTATCAACGCAGAGT	769
Oligo-dT_{30}N	AAGCAGTGGTATCAACGCAGAGTACT$_{30}$VN	770
TSO	AAGCAGTGGTATCAACGCAGAGTACATrGrG+G	771
CSFV F	CTAGCCATGCCCACAGTAGGA	772
CSFV R	CTCCATGTGCCATGTACAGCA	773

774 Underlining indicates NcoI and XhoI sequences.

775

776

777

778

779

780

781

782

783

784

bioRxiv preprint doi: https://doi.org/10.1101/389361; this version posted August 10, 2018. The copyright holder for this preprint (which was not certified by peer review) is the author/funder, who has granted bioRxiv a license to display the preprint in perpetuity. It is made available under aCC-BY-NC-ND 4.0 International license.

785 **TABLE 2**. Intermolecular force affecting the interaction of mAb HK44 and E2 proteins.

Intermolecular force	Amino acid
Conventional Hydrogen Bond	Arg64 (HC):Glu152 (E2)
	Ser145 (E2):Asp111Z (HC)
	Ala143 (E2):Asp34 (LC)
	Ser145 (E2):Asp111Z (HC)
	Pro146 (E2):Asp111Z (HC)
Carbon Hydrogen Bond	Thr147 (E2):Leu108 (LC)
	Thr147 (E2):Tyr116 (LC)
	Ser111B (HC):Thr88 (E2)
	Pro90 (E2):Tyr111 (HC)
Electrostatic (Attractive Charges)	Arg64 (HC): Glu152 (E2)
Electrostatic (Pi-Cation)	Arg150 (E2):Phe111X (HC)
Alkyl Hydrophobic	Pro146 (E2):Leu108 (LC)
	Val111A (HC):Pro90 (E2)
	His31(LC):Pro146(E2)
Pi-Sigma Hydrophobic	Tyr38(LC):Pro146(E2)
	Tyr110(HC):Ala143(E2)

786 HC: Heavy Chain; LC: Light Chain; E2: E2 protein.
787
788
789
790
791
792
793
794
795
796
797
798
799
800
801
802
803
804
805
806
807
808

bioRxiv preprint doi: https://doi.org/10.1101/389361; this version posted August 10, 2018. The copyright holder for this preprint (which was not certified by peer review) is the author/funder, who has granted bioRxiv a license to display the preprint in perpetuity. It is made available under aCC-BY-NC-ND 4.0 International license.

809 **TABLE 3.** Intermolecular force affecting the interaction of mAb HK24 and E2 proteins.

Intermolecular force	Amino acid
Conventional Hydrogen Bond	Ser36 (LC):Val144 (E2)
	Ser109 (LC):Thr147 (E2)
	Thr147 (E2):Leu114 (LC)
	Asn111A (HC):Gly87 (E2)
	Asn111A (HC):Asp86 (E2)
Carbon Hydrogen Bond	Ser36 (LC):Val144 (E2)
	Pro146 (E2):Ser109 (LC)
	Pro146 (E2):Ser28 (LC)
	Thr147 (E2):Leu114 (LC)
	Asn111A (HC):Gly87 (E2)
Alkyl Hydrophobic	Ala143 (E2):Cys111Y (HC)
	Pro146 (E2):Ile29 (LC)

810 HC: Heavy Chain; LC: Light Chain; E2: E2 protein.
811
812
813
814
815
816
817
818
819
820
821
822
823
824
825
826
827
828
829
830
831
832
833
834
835
836

bioRxiv preprint doi: https://doi.org/10.1101/389361; this version posted August 10, 2018. The copyright holder for this preprint (which was not certified by peer review) is the author/funder, who has granted bioRxiv a license to display the preprint in perpetuity. It is made available under aCC-BY-NC-ND 4.0 International license.

837 Fig. 1

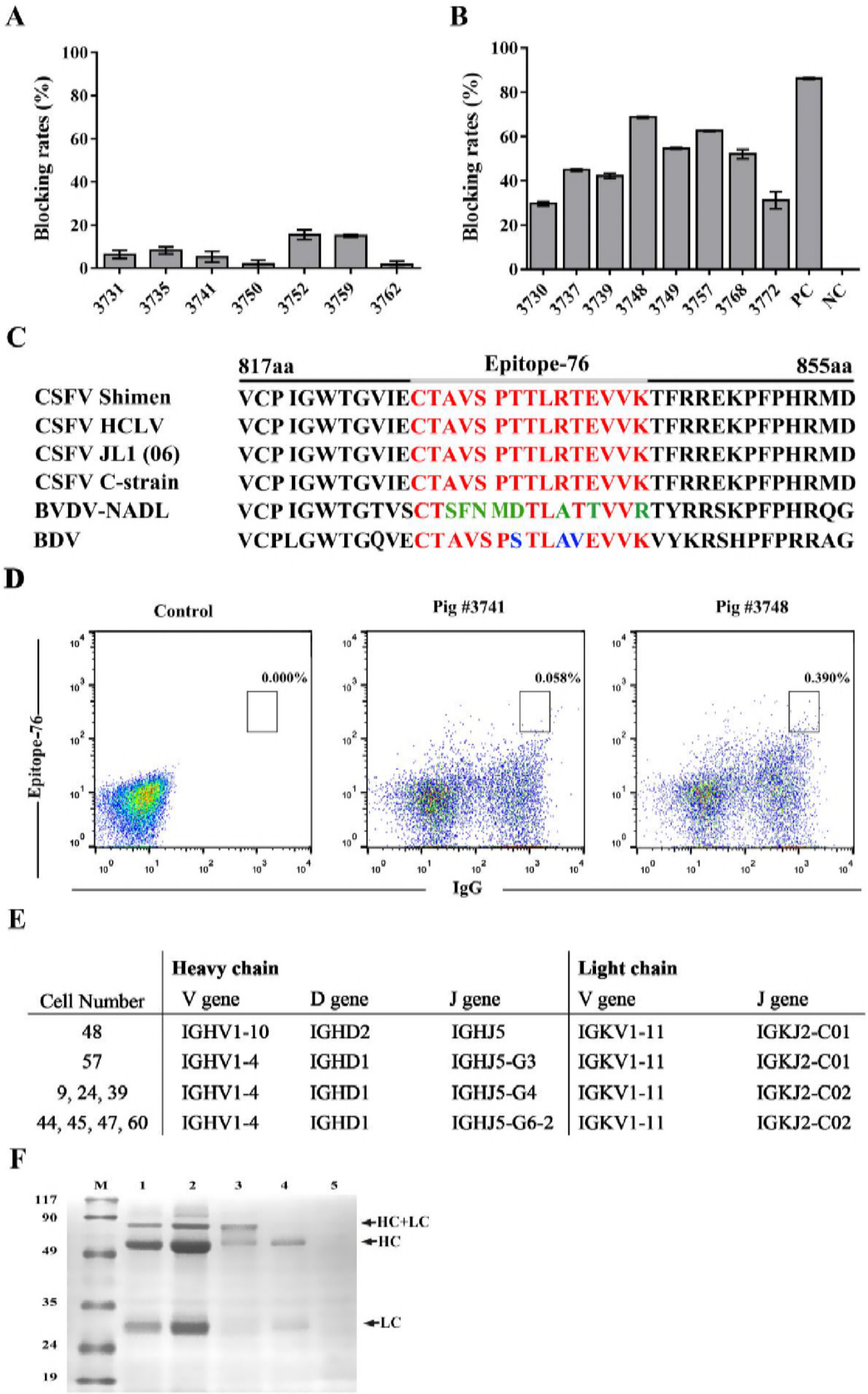

	Heavy chain			Light chain	
Cell Number	V gene	D gene	J gene	V gene	J gene
48	IGHV1-10	IGHD2	IGHJ5	IGKV1-11	IGKJ2-C01
57	IGHV1-4	IGHD1	IGHJ5-G3	IGKV1-11	IGKJ2-C01
9, 24, 39	IGHV1-4	IGHD1	IGHJ5-G4	IGKV1-11	IGKJ2-C02
44, 45, 47, 60	IGHV1-4	IGHD1	IGHJ5-G6-2	IGKV1-11	IGKJ2-C02

838

839

840

bioRxiv preprint doi: https://doi.org/10.1101/389361; this version posted August 10, 2018. The copyright holder for this preprint (which was not certified by peer review) is the author/funder, who has granted bioRxiv a license to display the preprint in perpetuity. It is made available under aCC-BY-NC-ND 4.0 International license.

841 Fig. 2

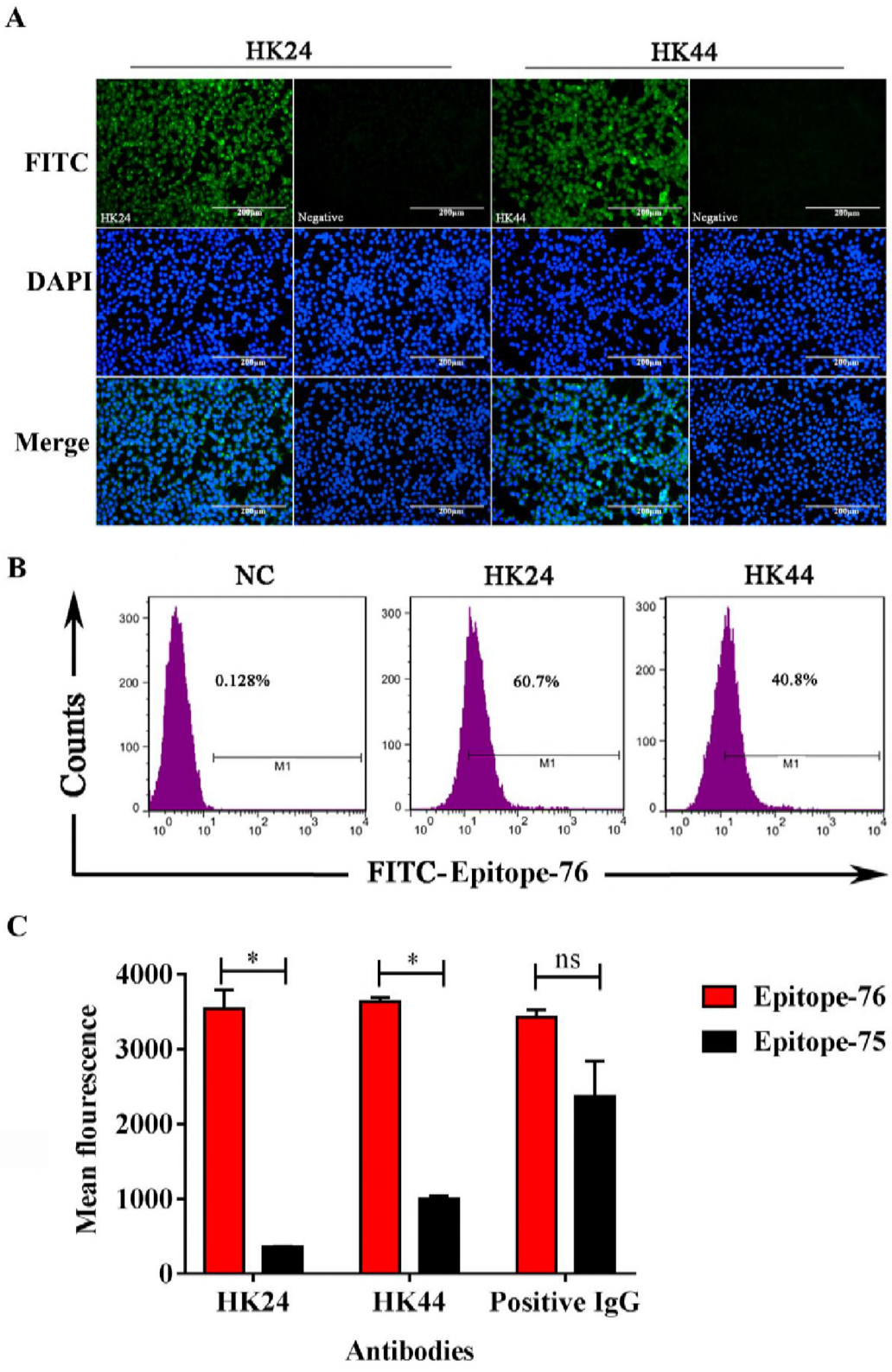

842

843

844

845

846

bioRxiv preprint doi: https://doi.org/10.1101/389361; this version posted August 10, 2018. The copyright holder for this preprint (which was not certified by peer review) is the author/funder, who has granted bioRxiv a license to display the preprint in perpetuity. It is made available under aCC-BY-NC-ND 4.0 International license.

847 Fig. 3

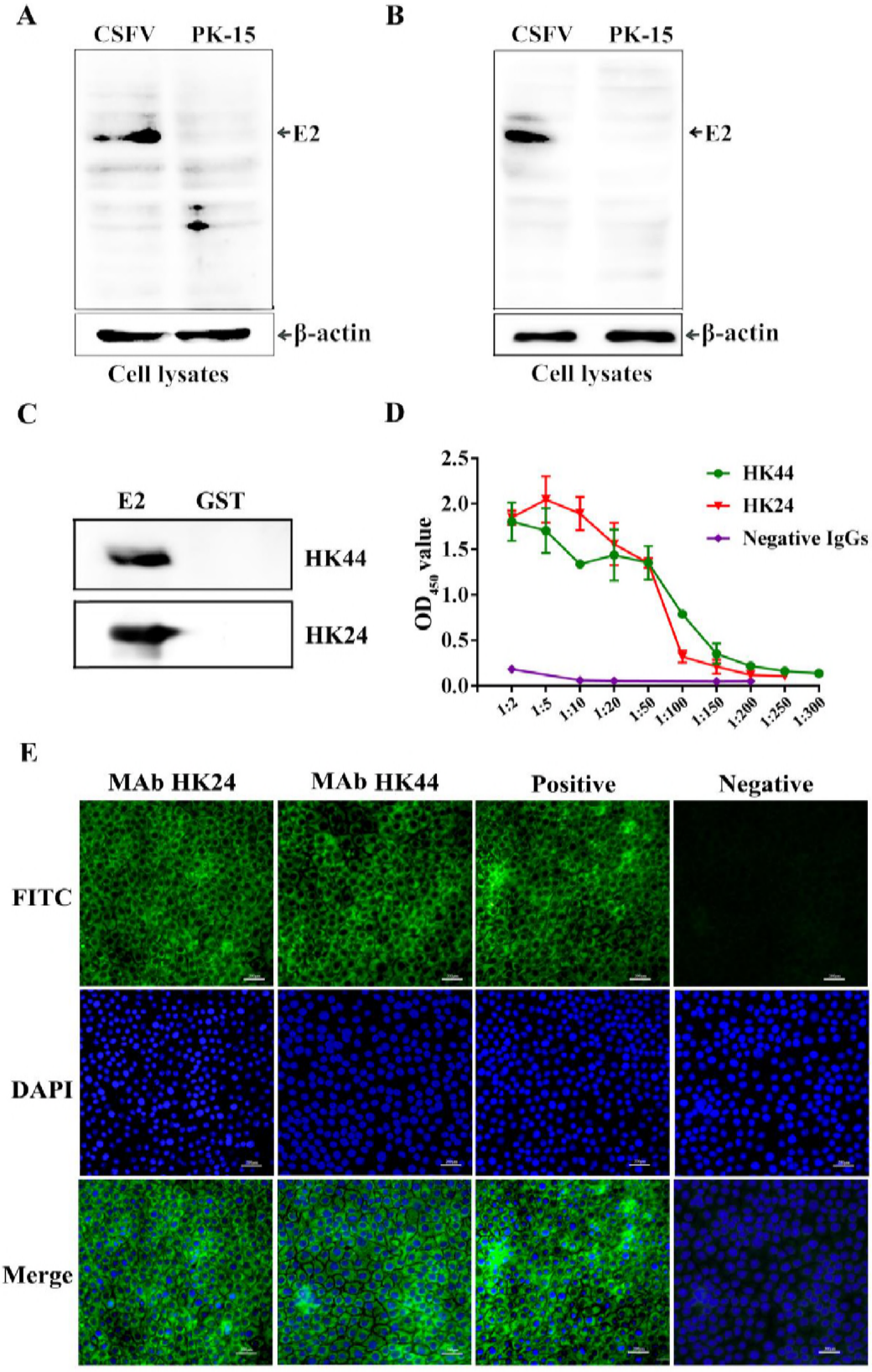

848

849

850

851

bioRxiv preprint doi: https://doi.org/10.1101/389361; this version posted August 10, 2018. The copyright holder for this preprint (which was not certified by peer review) is the author/funder, who has granted bioRxiv a license to display the preprint in perpetuity. It is made available under aCC-BY-NC-ND 4.0 International license.

852 Fig. 4

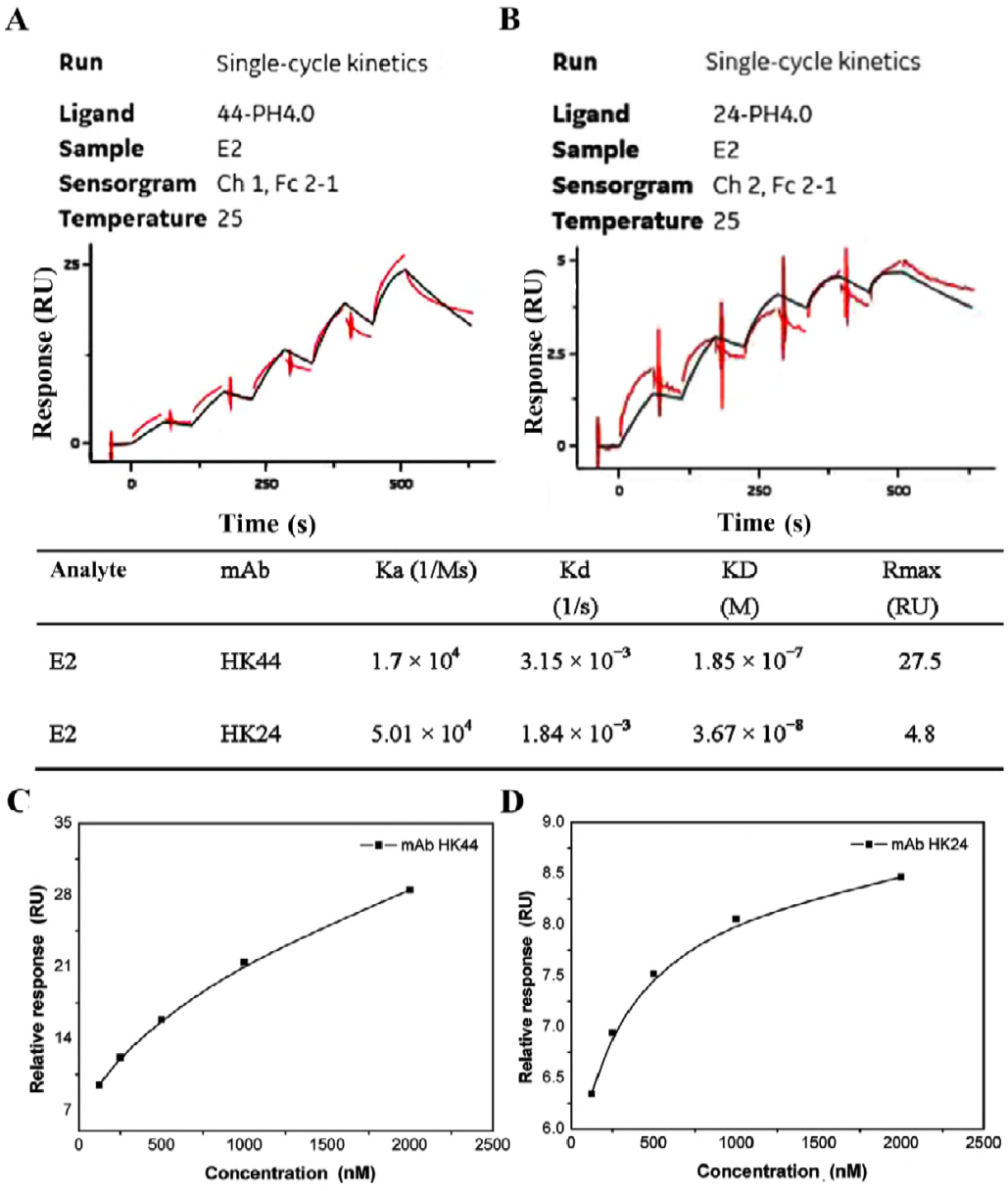

Analyte	mAb	Ka (1/Ms)	Kd (1/s)	KD (M)	Rmax (RU)
E2	HK44	1.7×10^{4}	3.15×10^{-3}	1.85×10^{-7}	27.5
E2	HK24	5.01×10^{4}	1.84×10^{-3}	3.67×10^{-8}	4.8

853
854
855
856
857
858
859
860
861
862
863
864
865
866

bioRxiv preprint doi: https://doi.org/10.1101/389361; this version posted August 10, 2018. The copyright holder for this preprint (which was not certified by peer review) is the author/funder, who has granted bioRxiv a license to display the preprint in perpetuity. It is made available under aCC-BY-NC-ND 4.0 International license.

867 Fig. 5

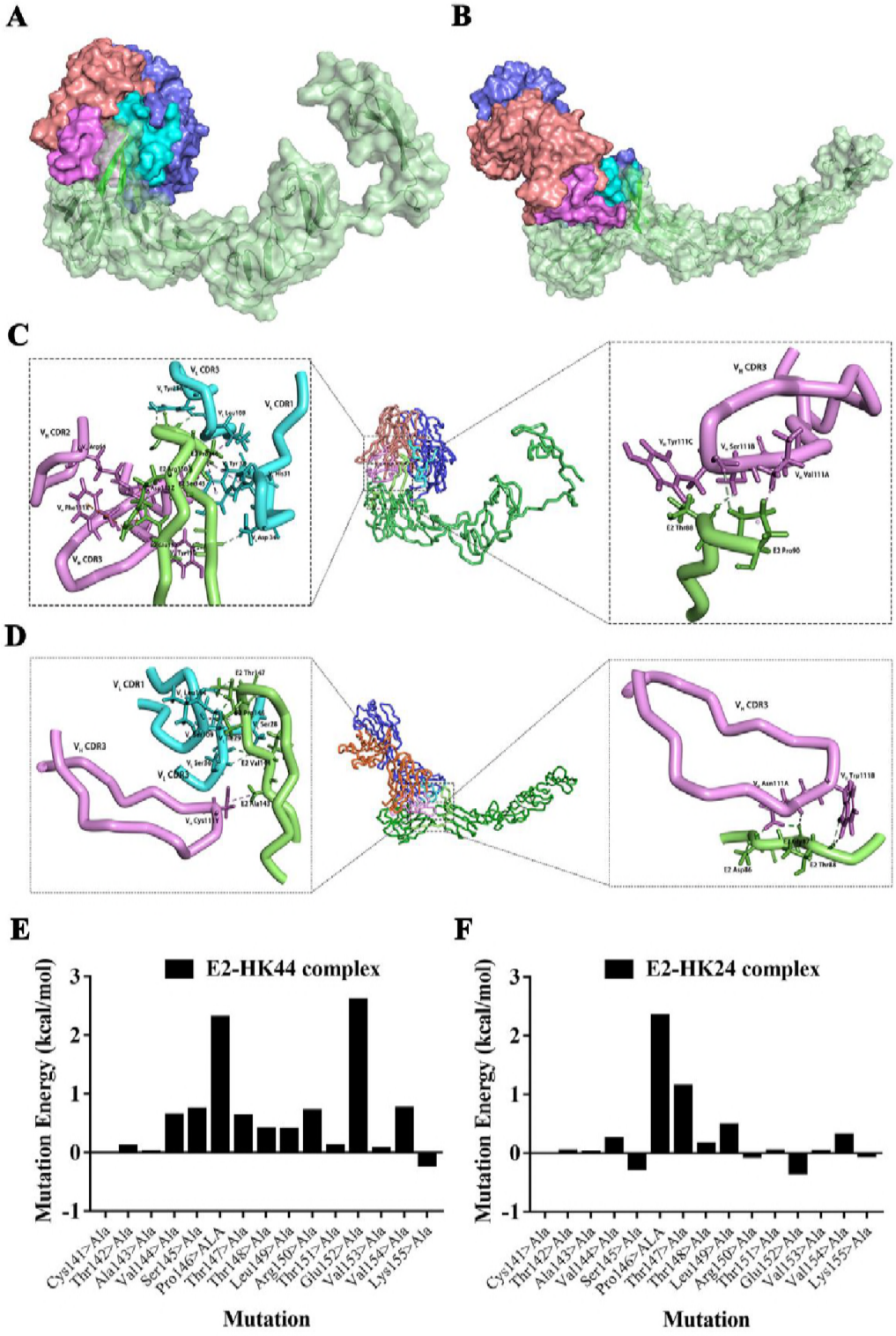

868

869

870

871

872

873

bioRxiv preprint doi: https://doi.org/10.1101/389361; this version posted August 10, 2018. The copyright holder for this preprint (which was not certified by peer review) is the author/funder, who has granted bioRxiv a license to display the preprint in perpetuity. It is made available under aCC-BY-NC-ND 4.0 International license.

Fig. 6

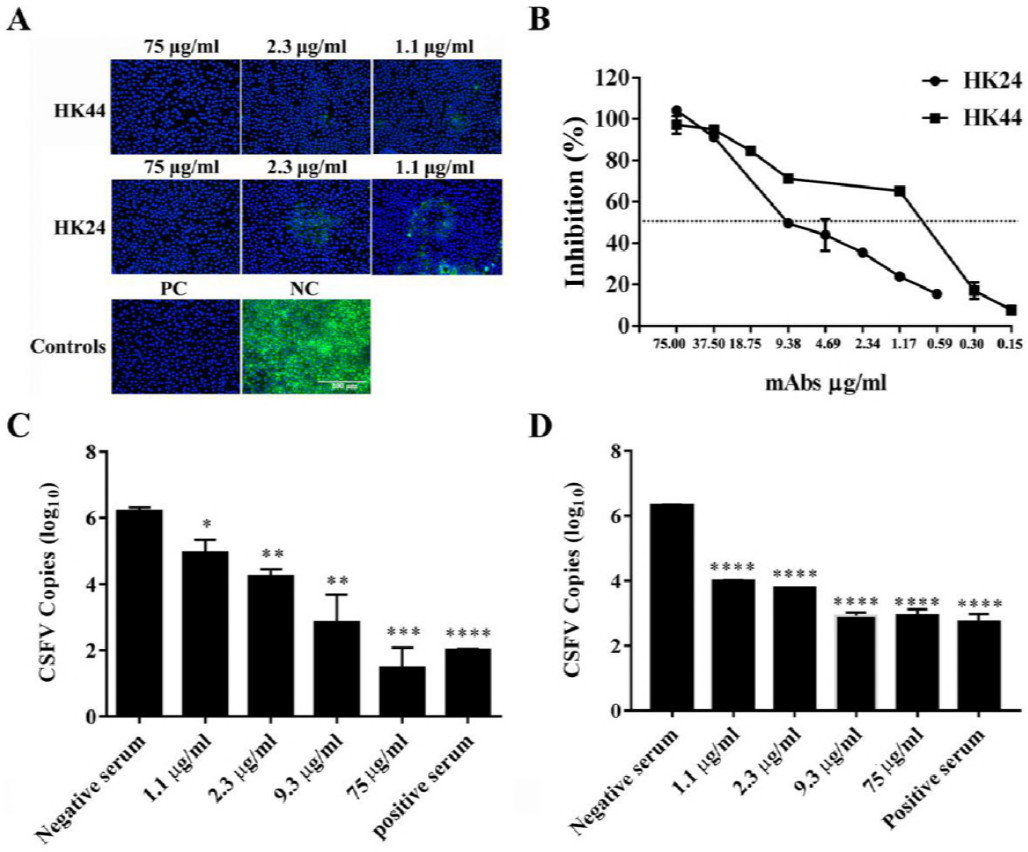

bioRxiv preprint doi: https://doi.org/10.1101/389361; this version posted August 10, 2018. The copyright holder for this preprint (which was not certified by peer review) is the author/funder, who has granted bioRxiv a license to display the preprint in perpetuity. It is made available under aCC-BY-NC-ND 4.0 International license.

Fig. S1

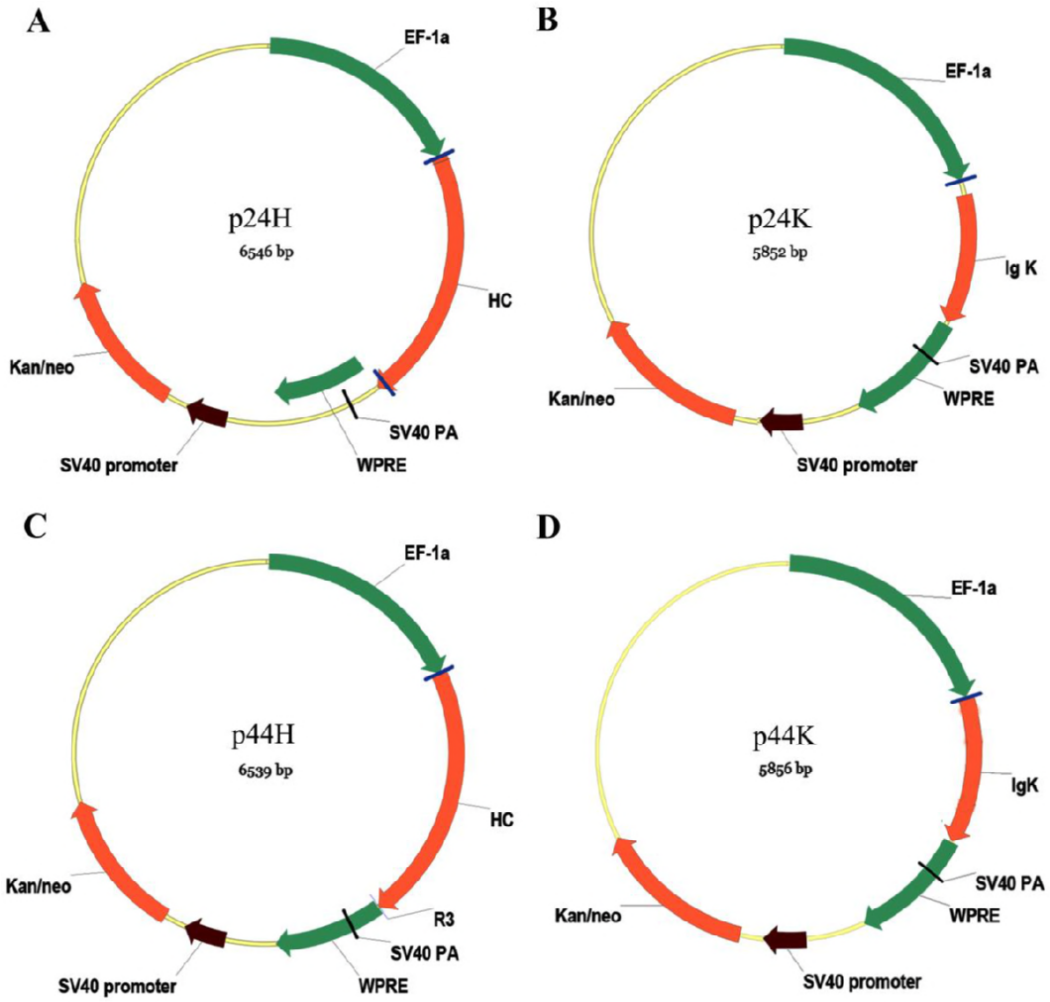

bioRxiv preprint doi: https://doi.org/10.1101/389361; this version posted August 10, 2018. The copyright holder for this preprint (which was not certified by peer review) is the author/funder, who has granted bioRxiv a license to display the preprint in perpetuity. It is made available under aCC-BY-NC-ND 4.0 International license.

938

939

940

941

942

943

944

945

946

947

948

949

950

951

952

953

954

955

956

957

958

959

960

961

962

963